Corrosion Resistance of Injection-Molded 17-4PH Steel in Sodium Chloride Solution

I. Costa,[‡,] C.V. Franco,[**] C.T. Kunioshi,[*] and J.L. Rossi[*]*

ABSTRACT

The corrosion resistance of 17-4PH powder injection-molded (PIM) martensitic stainless steel (SS) was evaluated in naturally aerated sodium chloride (NaCl) solution (3 wt%) at 25°C. This resistance was investigated by analyzing the curves of the evolution of open-circuit potential with time (E_{ocp} vs. time), electrochemical impedance spectroscopy (EIS), and surface observation by scanning electron microscopy (SEM) at increasing times of immersion. The susceptibility to pitting was investigated using cyclic potentiodynamic polarization curves and SEM observation after polarization. Additionally, the susceptibility to intergranular corrosion was evaluated by a modified procedure described in ASTM A 262 Practice A. The results of the 17-4PH PIM steel were compared to that of a 17-4PH steel produced by conventional metallurgy. The results showed that under steady-state conditions the PIM steel presented a behavior typical of passive metals during the whole test period (60 days of immersion). This was indicated by the E_{ocp} vs. time curves, EIS results, and SEM observation of the surface at increasing periods of immersion. The steel showed a bright metallic surface and no signs of corrosion during the whole period of the test. Cyclic potentiodynamic polarization curves indicated that both 17-4PH steels, conventional and PIM, are susceptible to pitting but the PIM steel showed a slightly increased susceptibility to pitting, which was supported by posttest observation by SEM. In the PIM steel, pits seemed to be related to the porosity that had inner oxide inclusions. The 17-4PH steel, produced by both PIM technology and conventional metallurgy, did not show a susceptibility to intergranular corrosion by ASTM A 262 Practice A.

KEY WORDS: electrochemical impedance spectroscopy, martensitic stainless steel, passive films, pitting corrosion, polarization

INTRODUCTION

Precipitation-hardenable (PH) steels are stainless steels (SS) that can be hardened by aging heat treatments. They are classified as austenitic, semiaustenitic, or martensitic steels. The 17-4PH (17Cr-4Ni) SS type belongs to the precipitation-hardened martensitic group.[1] It has a martensitic structure with low carbon content. After aging treatments its microstructure comprises tempered martensite and extremely fine, copper-rich intermetallic precipitates, whose properties depend on the aging temperature used. Heat treatment is straightforward and, with the exception of the solution treatment, is usually carried out at relatively low temperatures. The alloy is ferromagnetic, in both the solution-treated and aged states. The 17-4PH steel is one of the most widely employed precipitation-hardened SS, being commonly used in nuclear power plants, aircraft and gas turbines, oil and gas wells, and chemical process components owing to a combination of good mechanical properties and corrosion resistance at temperatures up to approximately 700°C. It also has a moderate corrosion resistance to salt spray atmosphere. Some of its properties, such as electrical resistivity, thermal expansion, and thermal conductivity are similar to those of austenitic and duplex steels, while its mechanical strength, after the

Submitted for publication June 2005; in revised form, November 2005.

‡ Corresponding author. E-mail icosta@ipen.br.
* IPEN/CNEN-SP, CCTM, Av. Lineu Prestes, 2242–Cidade Universitária, CEP 05508-000, São Paulo–SP, Brazil.
** LEC, Departamento de Química–CFM, Campus Trindade, CEP 88040-900–UFSC, Florianópolis–SC, Brazil.

0010-9312/06/000067/$5.00+$0.50/0

TABLE 1
Chemical Composition of 17-4PH Stainless Steels (wt%)

Stainless Steel	C	Si	Mn	P	S	Cr	Ni	Cu	Mo	Nb	Fe
17-4PH PIM	0.05	0.76	0.25	0.026	0.020	16.7	4.0	3.95	0.30	0.20	Rem.
17-4PH nominal	0.04 Max.	0.40 Max.	0.80 Max.	0.40 Max.	0.030 Max.	15.00 to 17.50	3.00 to 5.00	3.00 to 5.00	0.50 Max.	0.15 to 045	Rem.

aging heat treatment, is significantly superior to that of austenitic steels such as AISI 304[(1)] (UNS S30400)[(2)] or AISI 316 (UNS S31600).

The mechanical strength of 17-4PH steel increases after specific heat treatments that promote the precipitation of hardening phases such as å copper-rich and/or chromium rich α′.[2] It also presents high fatigue resistance in aggressive environments and can be used at temperatures ranging from –200°C to 480°C.

Some publications[1-3] have dealt with the corrosion aspects of these alloys produced by conventional metallurgy, such as general corrosion, pitting, and hydrogen embrittlement in an alkaline solution,[1] stress-corrosion cracking,[2] and crevice corrosion.[3] Lately, this steel has been produced using powder metallurgy (P/M) techniques. It is well known that the porosity present in P/M steels affect their corrosion resistance. This has been subject of particular interest from several recent investigations.[4-16] The porosity increases the area of metallic material exposed to the corrosive environment and might eventually induce crevice corrosion, with concentration cells within the pores. This reduces the passivity of the sintered alloy.[8-11] Recently, a new technique, known as powder injection molding (PIM), has been developed. Injection molding has been applied to powdered materials as an alternative route to manufacture corrosion-resistant sintered components. The PIM technology has been commercially used for manufacturing small components with a high degree of complexity.[17] The fundamental principles of this technique are closely related to microfusion and it represents a significant technological breakthrough in powder metallurgy. Fine powders (median particle size below 25 μm) are commonly used, resulting in sintered densities of about 98% of the theoretical density of the alloy. Injection-molded alloys generally include few and rounded pores. This microstructural feature improves the corrosion behavior of the material compared with conventionally sintered types. Injection-molded materials may be especially important for orthodontic components and surgical instruments where AISI 316L (UNS S31603) and 17-4PH steels have often been used.

The electrochemical behavior of AISI 316L PIM steel has been investigated in a NaCl solution.[15] Salt spray tests have been carried out with AISI 316L and 17-4PH PIM steels, the results being reported in a previous work.[16] The corrosion behavior of the 17-4PH PIM steel still, however, needs investigation and a full comprehensive study is not found in the literature. The aim of the present work is to investigate the corrosion resistance of 17-4PH steel produced by the PIM technology and to compare it to that of 17-4PH steel produced by conventional metallurgy. This behavior was evaluated by monitoring the open-circuit potential evolution along the time, electrochemical impedance spectroscopy (EIS), cyclic potentiodynamic polarization technique, and posttest surface inspection using scanning electron microscopy (SEM) at increasing periods of the test. Susceptibility to intergranular attack and pitting has also been evaluated in this study.

EXPERIMENTAL PROCEDURES

Material

Samples of powder injection-molded 17-4PH steel were used in this study. Presintering and debinding was performed at 980°C for 1 h under H_2 atmosphere. Sintering was carried out at 1,300°C for 4 h in a reducing atmosphere of hydrogen (pressure of 50 mmHg), followed by cooling in the furnace. The final density of the sintered material was 7.6 $g.cm^{-3}$. The density of the sintered material was approximately 98% of the theoretical density (7.8 $g.cm^{-3}$). This low porosity indicates the lack of interconnected porosity in this steel. Table 1 displays the chemical composition of the 17-4PH PIM steel used in this study in comparison to the nominal composition of the alloy. The carbon content in the sintered steel was 0.05 wt%, as indicated in Table 1, slightly above the specified amount (0.04 wt% maximum).

Microstructural Analysis

The microstructure of the studied steels was assessed using an SEM after surface preparation by grinding with 400, 600, 800, 1,200, and 2,000 grit emery paper, followed by polishing with diamond paste (6 μm and 1 μm) and finally the surface was attacked with Villela's solution.

[(1)] American Iron and Steel Institute (AISI), 1101 17th St. NW, Suite 1300, Washington DC 20036.
[(2)] UNS numbers are listed in *Metals and Alloys in the Unified Numbering System*, published by the Society of Automotive Engineers (SAE International) and cosponsored by ASTM International.

Specimen Preparation

The working electrodes were prepared by cold-resin mounting, and the surface ground with silicon carbide (SiC) paper up to #2000, followed by polishing with diamond paste (6 μm and 1 μm) to a mirror finish, then rinsing in deionized water and drying under a hot air stream prior to immersion in the test medium.

Test Medium

The experiments were performed in unstirred and naturally aerated 3 wt% NaCl electrolyte at a temperature of (25 ± 2) °C.

Electrochemical Methods

The electrochemical methods used in this investigation were open-circuit potential (E_{ocp}) measurements along with time, cyclic potentiodynamic polarization test, and EIS. The parameters of interest determined from the cyclic polarization curves were the corrosion potential (E_{corr}), the corrosion current density (i_{corr}), the pit protection potential (E_{prot}), the pitting or breakdown potential (E_b), and the passive current density (i_{pass}). A three-electrode cell arrangement was used for the electrochemical tests, with a platinum wire and a saturated calomel electrode (SCE) used as counter and reference electrodes, respectively. Cyclic potentiodynamic polarization tests were carried out using a 273A EG&G PAR potentiostat. The samples were scanned from –500 mV vs. E_{ocp} in the anodic (positive) direction with a scan rate of 1 mV/s. The scan was reversed when the current density increased by approximately 1,000 times, and it was stopped when the loop was completed. EIS measurements were accomplished using a Solartron 1260† frequency response analyzer coupled to a potentiostat electrochemical interface. EIS measurements were carried out in potentiostatic mode at the open-circuit potential (E_{ocp}), with a sinusoid ac voltage signal of amplitude 10 mV. The frequency range scanned was from 100 kHz down to 10 mHz, with 10 points per decade. The experiments were carried out at increasing periods of immersion time, from 1 to 60 days of immersion. All electrochemical and immersion tests were carried out in triplicate to evaluate the repeatability. The results obtained in this work showed good repeatability and the data presented here are representative of all.

Surface Inspection

The surfaces of the steel were observed before and after the immersion test and also after the polarization test by SEM.

Sensitization Evaluation

The susceptibility of the 17-4 PH steels to intergranular attack was evaluated using the ASTM A 262 test for both the PIM and conventional conditions.[18] Specimens of these steels were tested using practice A modified (electrolytic etching using ammonium persulfate [$(NH_4)_2S_2O_8$]) after heat treatment at 675°C for 1 h. The ASTM A 262 practice A modified version is usually used for Mo-containing SS.

† Trade name.

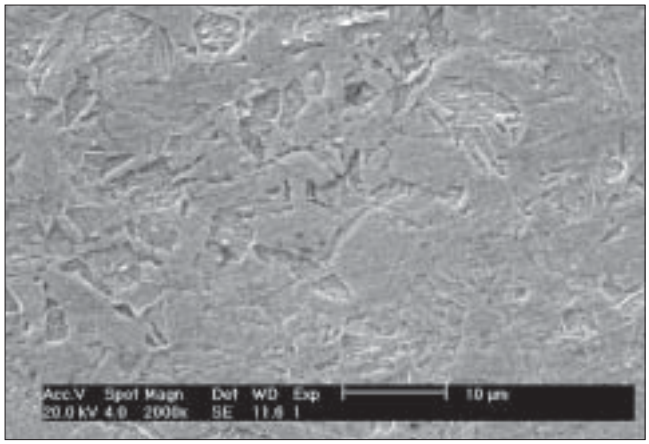

(a)

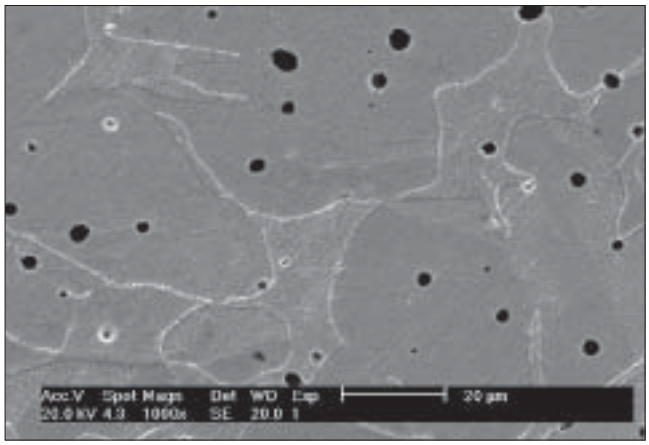

(b)

FIGURE 1. *Microstructures of the 17-4PH steels produced by (a) conventional metallurgy and (b) PIM steel. Etchant Villela's solution.*

RESULTS

The microstructures of the 17-4PH steels, as received, PIM and conventional, observed using a SEM are shown in Figure 1. The 17-4PH conventional steel shows a predominantly martensitic microstructure with small grains. The 17-4PH PIM steel reveals large grains with an inner martensitic structure and rounded pores. The large grains might have been the result of the high temperatures used during the presintering and sintering processes.

Sensitization Evaluation

In this procedure, electrolytic etching was carried out using $Na_2S_2O_8$. SEM micrographs from 17-4PH

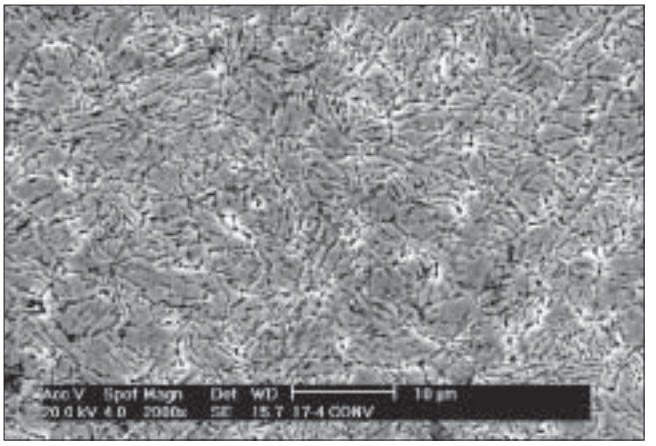

(a)

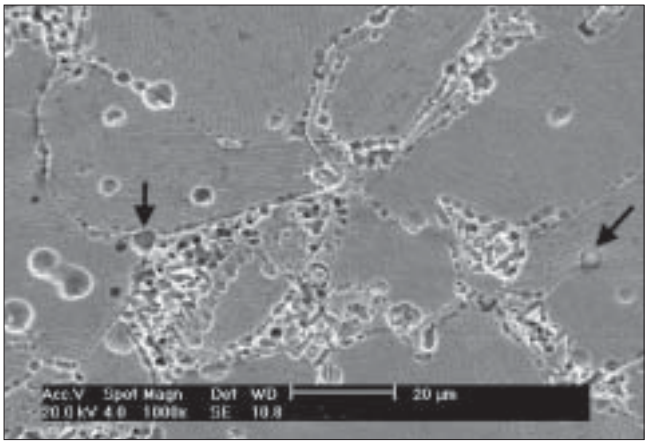

(b)

FIGURE 2. *SEM micrographs of 17-4PH steels after heat treatment (675°C for 1 h) and electrolytic etching with $(NH_4)_2S_2O_8$. (a) conventional metallurgy steel and (b) PIM steel.*

PIM and conventional steels, after heat treatment at 675°C for 1 h and electrolytic etching, are shown in Figure 2. The 17-4PH conventional steel still shows a predominantly martensitic microstructure after the heat treatment and no intergranular attack was observed. The 17-4PH PIM steel after heat treatment and electrolytic etching reveals preferential attack at some regions, either at or near the grain boundaries, but no intergranular attack was observed. Shallow pits can also be seen on the surface, away from the regions of preferential attack. Rounded pores and spherical particles (indicated by arrows on the figures) can be seen inside some of the pores. X-ray dispersive energy spectroscopy (EDS) revealed that those particles are silica (SiO_2), possibly trapped inside the pores during the manufacturing process, confirming results from other investigations.[19-20] The chemical composition of the PIM material (see Table 1) also shows that there was a high level of silicon present. Some of these silica particles might have been removed from the pores either by mechanical polishing or electrolytic etching. The average grain size of the PIM steel after heat treatment was 43 ± 4 µm. The etched structure of the 17-4PH steel, whether conventionally produced or injection-molded, showed that both 17-4PH steels had no susceptibility to intergranular attack.

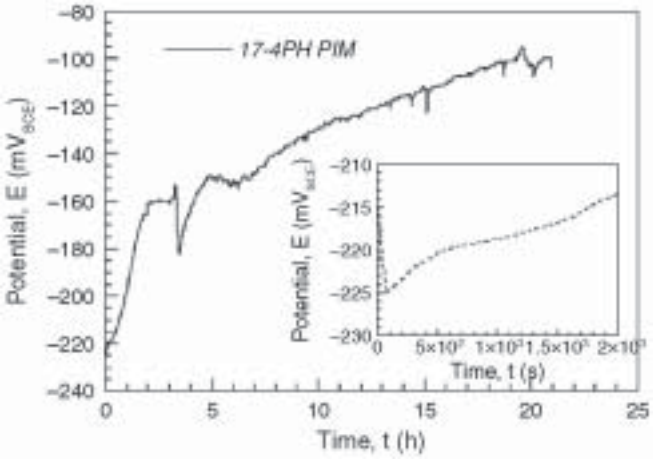

FIGURE 3. *(E_{ocp} vs. time) for 17-4PH PIM steel in naturally aerated NaCl (3 wt%) solution at 25°C.*

Open-Circuit Potential vs. Time

Figure 3 shows the E_{ocp} variation with time for a 21-h period for the 17-4PH PIM steel in naturally aerated NaCl solution. Immediately after immersion the E_{ocp} was approximately –215 mV_{SCE}. In the first minutes of immersion E_{ocp} dropped to –225 mV_{SCE} but soon afterwards it increased, until after 2 h a steady potential of approximately –160 mV_{SCE} was reached. The steady potential was maintained for only about 1 h and then a potential drop to –180 mV_{SCE} occurred, followed by a potential increase that demonstrated a logarithmic relationship with time for up to 1.5 h. From 5 h to 19 h the tendency observed was to increase in the E_{ocp}, and during this period a number of oscillations occurred. Between 19 h and 21 h the potential still showed a few oscillations around a mean value of approximately –100 mV_{SCE} with amplitude of nearly 10 mV. A period of 20 h was therefore allowed for stabilization of the potential before EIS was applied.

Electrochemical Impedance Spectroscopy

Impedance spectra obtained at increasing times in the NaCl solution allowed the monitoring of the evolution of the electrochemical behavior of the 17-4PH PIM steel with time. No significant changes were found in the EIS diagrams from the first days of immersion up to 15 days. From 15 days to 60 days, the EIS results indicated a slight increase in the impedance of the 17-4PH PIM steel, as indicated in Figure 4. The Bode phase diagram corresponding to 15 days of the test shows from medium frequencies (MF) to low frequencies (LF), a large peak near –90° suggesting a

highly capacitive behavior indicative of the presence of a passive oxide layer on the steel surface, Figure 4(a). This highly resistant film on the PIM steel surface was apparently maintained on the surface until the end of the test (60 days after immersion), under steady-state conditions. The slight increase seen in the impedance modulus at low frequencies, from 15 days to 60 days, Figure 4(b), is likely to be caused by a thickening of the passive film, as the E_{ocp} evolution with time indicated for the first hours of immersion.

SEM images of the 17-4PH PIM steel surface, before immersion and at increasing times of the test (14 days, 30 days, and 60 days of test) are shown in Figure 5. The surface of the 17-4PH PIM steel did not show variations or any signs of corrosion as the immersion time increased.

At 60 days of the test the PIM steel surface was still shiny, indicating passive behavior for the 17-4PH PIM steel in the NaCl (3 wt%) solution during the whole test period. As reported above, the round porosity is a feature of the fabrication process (P/M technology) and the spherical particles inside the pores, indicated by arrows, are mainly SiO_2, as demonstrated by EDS analysis. The porosity might act as pit nucleation sites, and the oscillations in the corrosion potential during the first hours of immersion indicated that pits nucleated on the surface but were unstable and appeared to repassivate. In fact, pits were not observed in the 17-4PH PIM steel, even after 60 days of the test under steady-state conditions.

Cyclic Potentiodynamic Polarization Test

Figure 6 shows the typical cyclic potentiodynamic polarization curve of the 17-4PH conventional and PIM steels, in NaCl (3 wt%) solution. The E_{ocp} after approximate stabilization (E_{corr}) obtained from these curves was approximately –310 mV_{SCE} for the conventional steel and –358 mV_{SCE} for the PIM steel. From the corrosion potential to approximately –175 mV_{SCE}, the polarization curve for the 17-4PH PIM steel was indicative of a poorly protective film. The slope here probably reflects a balance between the high scan rate and the relatively slow response of passive film growth. At about –175 mV_{SCE} a change in the anodic slope occurs and at approximately –75 mV_{SCE} a small peak was seen. From potentials of approximately 10 mV_{SCE} to higher potentials, the current density largely increases, indicating a breakdown of the passive film. This is the critical pitting potential (E_b). The potential was reversed when the current density increased by three orders of magnitude. The potential at which the reverse anodic scan meets the passive region and the loop is closed, is referred here as the pit protection potential, E_{prot}. The value of E_{prot} estimated from the polarization curve for the PIM steel was approximately –180 mV_{SCE}.

The values of i_{corr} were estimated approximately by extrapolating the cathodic part of polarization

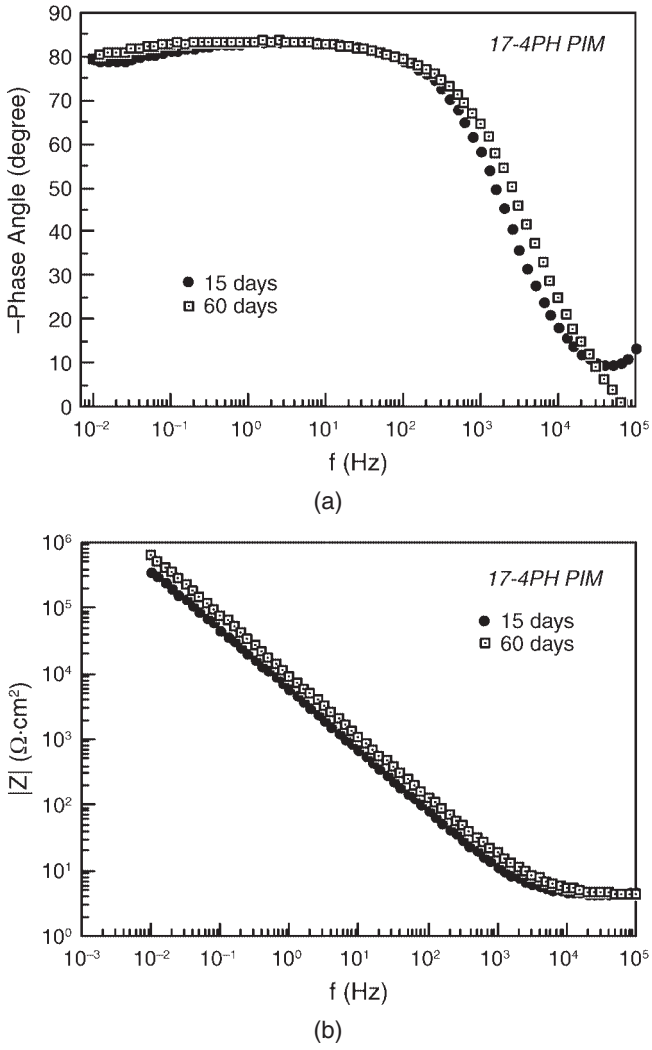

FIGURE 4. *Bode diagrams from EIS of 17-4PH PIM steel for 15 days and 60 days of immersion time in NaCl solution (3 wt%).*

curves to E_{corr}. The i_{corr} estimated for the PIM steel is very low (6×10^{-7} A cm^{-2}) and typical of passive metals. However, the indication of an active behavior by the increase in i_{corr} with applied potential for this type of steel suggests that the passive layer on this steel is not highly resistant, permitting the partial dissolution of the steel, at least at weak sites of the surface film.

The polarization curve of the conventional 17-4PH steel, from –250 mV_{SCE} to approximately –100 mV_{SCE}, displayed an essentially passive behavior with i_{pass} of approximately 3×10^{-7} A cm^{-2}. At potentials above –100 mV_{SCE} i_{corr} slowly increased, suggesting the attack of the passive film, but only at potentials around 190 mV_{SCE} did a breakdown of the passive film occur.

Comparing the polarization curves for the PIM and conventional steels, it can be noticed that the conventional steel had lower current densities in the whole range of potentials. The E_b and the E_{prot} for the

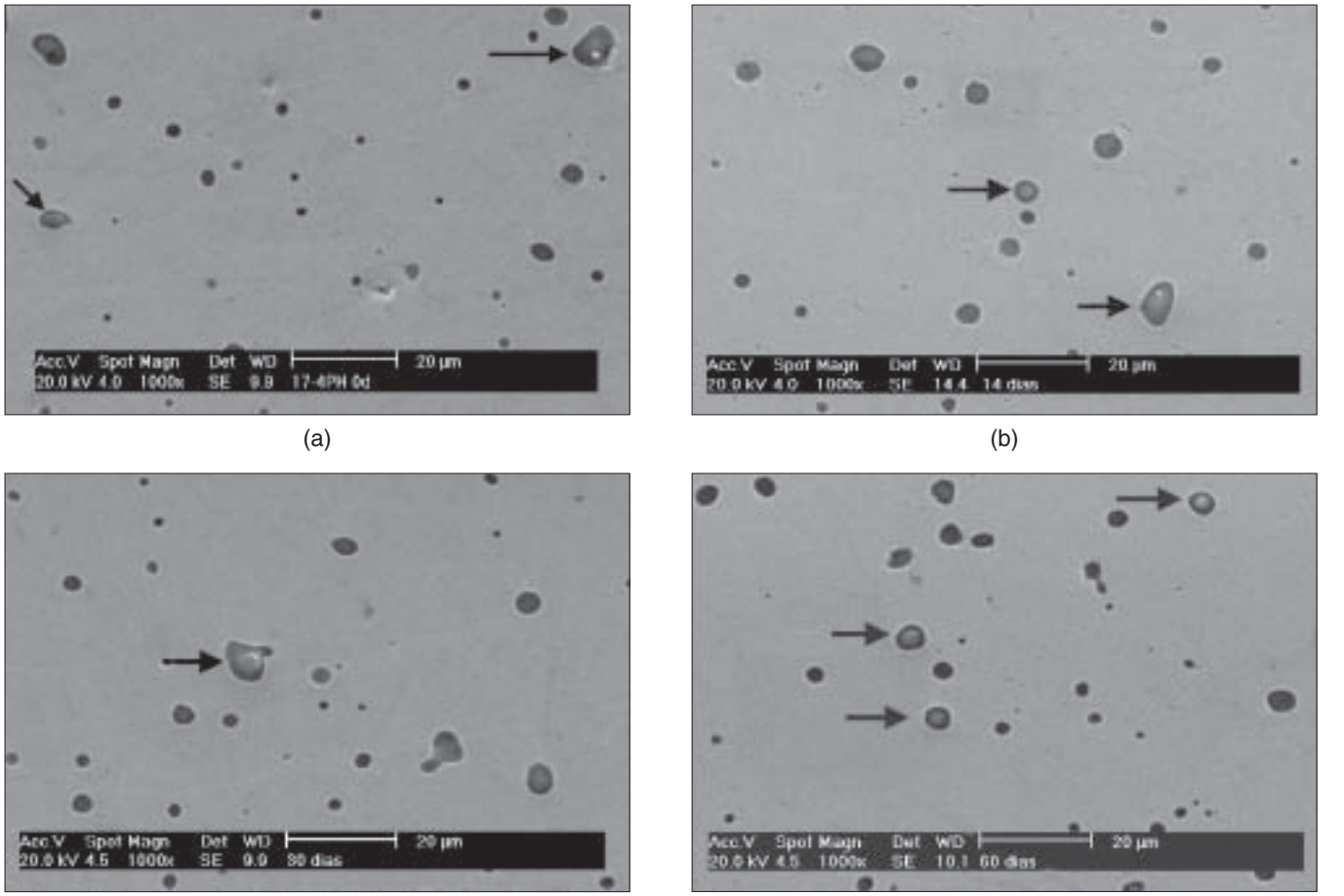

FIGURE 5. *SEM micrographs of the 17-4PH PIM steel surface before (a), and after (b) 14 days, (c) 30 days, and (d) 60 days of immersion time in NaCl solution (3 wt%). Arrows are pointing to silica particles inside porosity.*

conventional steel, approximately 200 mV_{SCE} and –115 mV_{SCE}, respectively, were well above that for the PIM steel, showing the increased pitting resistance of the conventional steel compared to the PIM type. This is caused by a more protective film on the conventional steel. The i_{corr} value estimated from the polarization curve for the conventional steel was 1.5×10^{-7} A cm^{-2}, that is, of the same order as that for the PIM steel.

SEM observation of the surfaces of the conventional and PIM steels, after polarization tests, showed pits on both types of steel, as Figure 7 shows. However there were fewer pits on the conventional steel (Figure 7[a]) than on the PIM type (Figure 7[b]). The pits on of the PIM steel showed irregular shapes, similar to those formed in austenitic steels.[15,21] Pits related to the 17-4PH steel fabricated by conventional metallurgy had a more regular morphology than those for the PIM steel, Figure 7. Differences were also found at the bottom of the pits for both types of steel, Figure 8. For the conventional steel, a large number of small particles were found in the pits (Figure 8[a]). These could have been either second phase particles, nobler than the matrix, or precipitates originated from the corrosion attack (corrosion products). At higher magnification (Figure 8[b]) it can be seen that these particles present a regular shape (round) with a diameter of less than 1 µm. For the PIM steel, round silica particles, of the same type found inside the porosity, can be seen at the bottom of the pits (Figure 8[c]).

DISCUSSION

The behavior shown in Figure 3 for the 17-4PH PIM steel is typical of passive metals immersed in aerated solutions, the corrosion potential being defined by the intersection of the passive anodic curve with the cathodic curve of the oxygen reduction reaction, in the range where it shows activation polarization.[22] It is proposed that the initial potential drop must have resulted from a partial dissolution of the air-formed passive film. This drop was followed by an increase in potential, possibly caused by thickening of the passive film and a reduced i_{pass}. The intersection of the cathodic curve with the passive straight line then shifted to higher potentials and consequently the corrosion potential increased. The increase in potential contin-

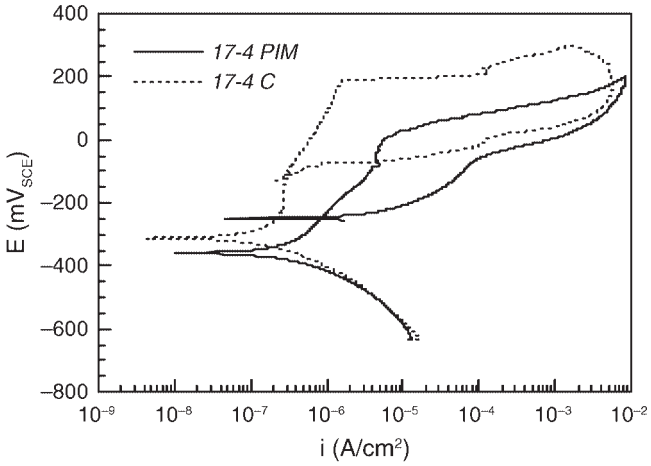

FIGURE 6. *Cyclic potentiodynamic polarization curves of 17-4PH steels produced by PIM and conventional metallurgy.*

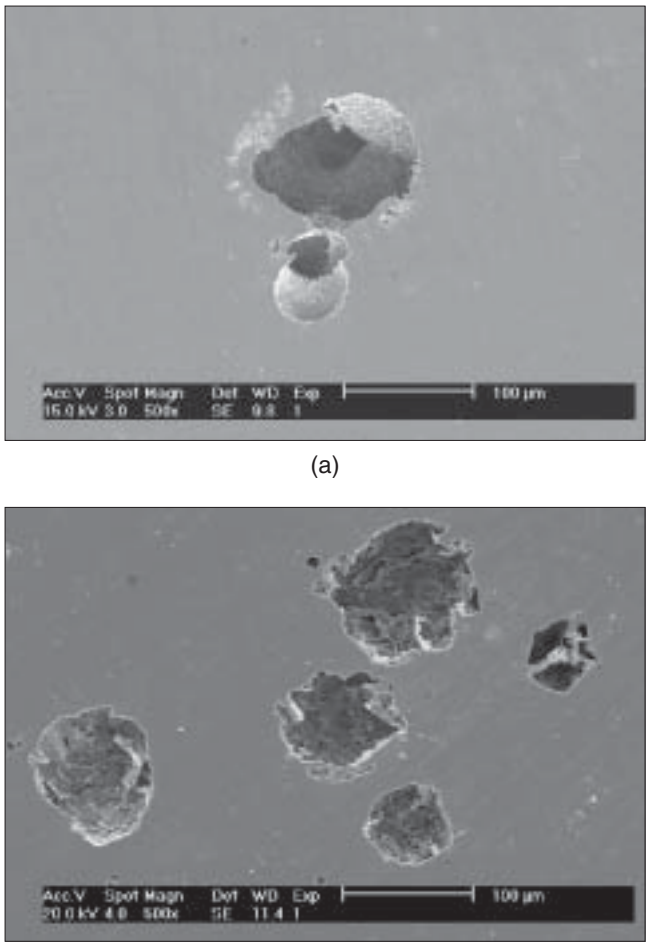

(a)

(b)

FIGURE 7. *SEM micrographs of 17-4PH steels after cyclic potentiodynamic polarization showing pits. (a) conventional and (b) PIM steel. A larger number of pits are seen on the surface of the PIM steel.*

ued until the passive film attained its limiting protective capacity, when the potential reached approximate stabilization.

The oscillations observed on the E_{ocp} vs. time curve suggests the occurrence of passive film breakdown followed by repair, in a similar way as for pit nucleation and repassivation, represented by a sudden drop in potential followed by an exponential increase with time. These results indicate the aggressive attack of the chloride ions toward the passive layer leading to pits that appear to be unstable but which tend to repassivate under steady-state conditions.

The EIS results showed a highly capacitive behavior from medium to low frequencies, typical of passive metals, and this was maintained during the whole period of the test. The impedance increased slightly from 15 days to 60 days of immersion (Figure 4). It is proposed that this increase must have been caused by a further and slow thickening of the passive film that was more clearly indicated by the E_{ocp} variation with time during the first hours of immersion (Figure 3).

Surface observation at increasing times of immersion (Figure 5) supported the results from EIS measurements that indicated passive behavior for the 17-4PH PIM steel during the whole test period.

The polarization curves of both 17-4PH steels showed similar shapes. Both presented a breakdown potential, E_b. For the PIM steel the E_b was around 10 mV_{SCE}, considerably lower than for the conventional steel, 190 mV_{SCE}. At potentials above E_b, pitting was established for both steels. The main differences between the two curves (Figure 6) are primarily the indication of a poorly protective film for the PIM steel at low overpotentials, and the increased current density values related to this steel, in the whole range of anodic polarization. The increase in current with the applied potential for the PIM steel at low overpotentials is indicative of a slow transformation of the passive film (relative to the scan rate) caused by passive film attack at weak areas and/or the permeability of the passive film. The more susceptible areas of the passive film to attack are regions of discontinuities or defects that could be related to the porosity and to the silica particles present in the PIM steel. Moreover, the decreased E_b and E_{prot} values for the PIM steel compared to the conventional type, suggests an increased susceptibility to pitting, which for the PIM steel is indicative of a less protective passive layer than for the conventional steel.

As mentioned above, the increased pitting susceptibility of the PIM steel is probably related to porosity and the silica particles inside the porosity. Exposed porosity is expected to increase susceptibility to pitting/crevice corrosion, lowering the pitting resistance of the PIM steel. The oxygen content inside the porosity, and particularly underneath the silica particles, will be insufficient to repair the surface oxide after it has been attacked. Corrosion cells might be

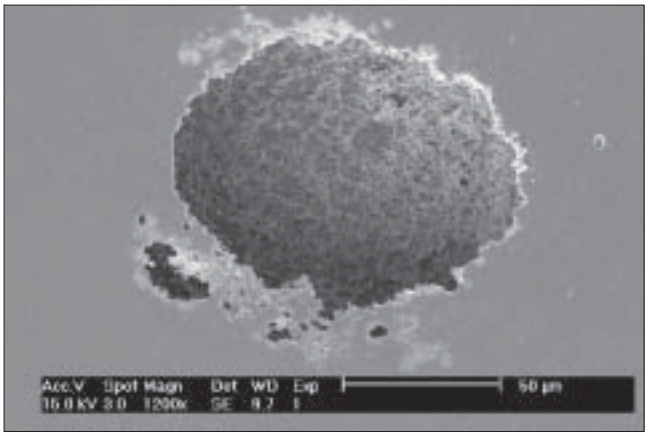

(a)

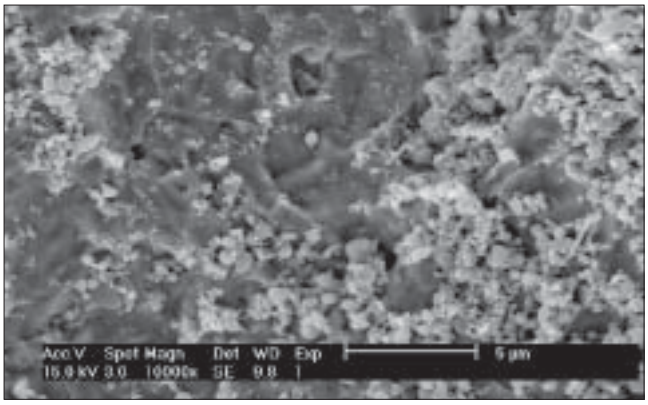

(b)

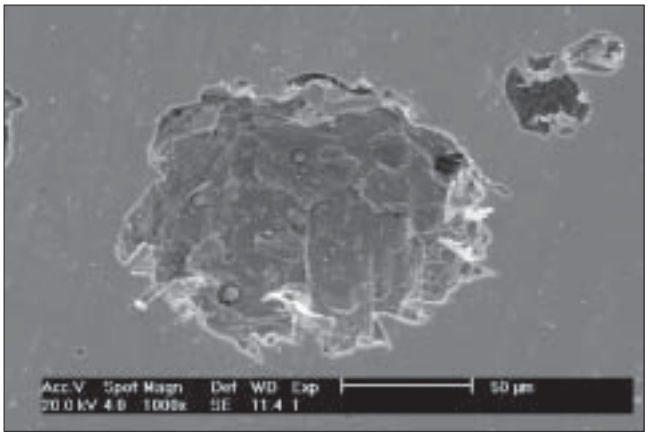

(c)

FIGURE 8. *SEM micrographs showing the bottom of the pits for 17-4PH steels (a) prepared by conventional metallurgy, (b) same as in (a) at higher magnification, and (c) prepared by PIM.*

established between the shielded portion (underneath the silica particles) and the unshielded metallic surface (cathode). The dependence of the current density with the applied potential, at potentials larger than the pitting critical potential, is indicative of a behavior typical of crevice corrosion. In this case, porosity might act as crevices in the steel. The high availability of oxygen at the metallic surface of the steel produced by conventional metallurgy, on the other hand, results in lower i_{pass} and higher E_b comparative to the 17-4PH PIM steel.

Other evidence of the increased susceptibility to pitting of the PIM steel compared with the conventional steel was the higher density of pits for the former, found after polarization, which seemed to be related to the porosity with silica particles in the PIM steel. It has been previously proposed that silica particles trapped inside the pores might promote pit initiation.

The corrosion potential obtained from the polarization curve for 17-4PH PIM steel, –360 mV_{SCE}, was much lower than that measured by open-circuit measurements, –100 mV_{SCE}. The reason for this difference is that the polarization test started at a cathodic potential well below the potential measured at open circuit. This is often the case in dynamic measurements due to local solution chemistry changes at the surface and relatively slow transformation of the passive film. Under steady-state conditions at the E_{ocp}, pits were not seen on the surface of the PIM steel, even after long periods of immersion time (60 days), and the results indicated a build-up of passive film in this solution. The low values of i_{corr} obtained from the polarization curve for the 17-4PH PIM steel in the NaCl solution also support the presence of a passive film associated with this steel.

CONCLUSIONS

❖ Results from the cyclic polarization curves indicate that the film formed on the PIM steel is not as protective as that on the steel produced by conventional metallurgy.
❖ A comparison of the 17-4PH steels fabricated by the two methods, conventional metallurgy and PIM, also indicates an increased tendency toward pitting related to the 17-4PH PIM steel.
❖ Susceptibility to intergranular corrosion was not found for either of the two types of 17-4PH steel evaluated.
❖ The 17-4PH PIM steel shows a passive behavior under steady-state conditions at open-circuit potential but eventually unstable pits might nucleate and repassivate. Results from open-circuit potential variation with time, electrochemical impedance spectroscopy, and surface observation by SEM at increasing times support these results.
❖ EIS data show a capacitive response from medium to low frequencies typical of passive materials during the whole test period.

ACKNOWLEDGMENTS

The authors are grateful to LUPATECH for providing the 17-4PH PIM steel for investigation.

REFERENCES

1. H.J. Chuang, S.Y. Chen, S.L.I. Chan, Corros. Sci. 41 (1999): p. 1,347-1,358.
2. F. El Hilali, M. Habashi, A. Mohsine, Annal. Chem. Sci. Mater. 24 (1999): p. 169-194.
3. A.U. Malik, N.A. Siddiqi, S. Ahmad, I.N. Andijani, Corros. Sci. 37, 10 (1995): p. 1,521-1,535.
4. P.C. Borges, N.C. Pereira, C.V. Franco, A.N. Klein, Adv. Powder Metall. Particul. Mater. 2 (1994): p. 61.
5. N.C. Pereira, F.G. Mittelstadt, A. Spinelli, C.V. Franco, A.M. Maliska, A.N. Klein, J.L.R. Muzart, J. Mater. Sci. 30 (1995): p. 4,817.
6. A.V.C. Sobral, A.M. Maliska, G. Tosi, J.L.R. Muzart, A.N. Klein, C.V. Franco, Adv. Powder Metall. Particul. Mater. 3, 11 (1995): p. 57.
7. A.V.C. Sobral, A.C.B. Parent, J.L.R. Muzart, C.V. Franco. Surf. Coat. Technol. 92 (1997): p. 10.
8. E. Maahn, S.K. Jensen, R.M. Larsen, T. Mathiesen, Adv. Powder Metall. Particul. Mater. 7 (1994): p. 253.
9. L. Fedrizzi, F. DeFlorian, A. Tiziani, Adv. Powder Metall. Particul. Mater. 7 (1994): p. 273.
10. T. Raghu, S.N. Malhotra, P. Ramakrishnan, Br. Corros. J. 2 (1988): p. 109.
11. A. Tremblay, R. Angers, Adv. Powder Metall. Particul. Mater. 7 (1995): p. 225.
12. E. Otero, A. Pardo, M.V. Utrilla, F.J. Pérez, C. Merino, Corros. Sci. 39 (1997): p. 453.
13. E. Klar, F.K. Samal, Adv. Powder Metall. Particul. Mater. 11 (1995): p. 11.
14. R.L. Sands, G.F. Bidsmesd, D.A. Oliver, Mod. Dev. Powder Metall. 2 (1966): p. 73.
15. A.V.C. Sobral, W. Ristow Jr., D.S. Azambuja, I. Costa, C.V. Franco, Corros. Sci. 43, 6 (2001): p. 1,019-1,030.
16. A.V.C. Sobral, W. Ristow Jr., O.V. Correa, C.V. Franco, I. Costa, Key Eng. Mater. 189-191 (2001): p. 667-672.
17. T. Mathiesen, E. Maahn, Adv. Powder Metall. Particul. Mater. 3 (1995): p. 45-55.
18. ASTM A262-81, "Standard Practices for Detecting Susceptibility to Intergranular Attack in Austenitic Stainless Steels," in Annual Book of ASTM Standards (West Conshohocken, PA: ASTM International, 1981).
19. D.D. Macdonald, H. Song, K. Makela, K. Yoshida, Corrosion 49 (1993): p. 8.
20. I. Sekine, Corros. Sci. 32 (1991): p. 815.
21. D.C. Silverman, J.E. Carrico, Corrosion 44 (1988): p. 280.
22. I.C. Lavos-Valereto, I. Costa, S. Wolynec, J. Biomed. Mater. Res. 63, 5 (2002).

CORROSION RESEARCH CALENDAR

Corrosion is a technical research journal devoted to furthering the knowledge of corrosion science and engineering. Within that context, *Corrosion* accepts notices of calls for papers and upcoming research grants, meetings, symposia, and conferences. All pertinent information, including the date, time, location, and sponsor of an event should be sent as far in advance as possible to: Angela Jarrell, Managing Editor, *Corrosion*, 1440 South Creek Drive, Houston, TX 77084-4906. Notices that are not accompanied by the contributor's name, daytime telephone number, and complete address will not be considered for publication.

2006

April 23-26—3rd International Brazing and Soldering Conference—San Antonio, TX; Contact Customer Service, Phone: +1 440/338-5151, ext. 6; E-mail: cust-srv@asminternational.org; Web site: www.asminternational.org/ibsc.

April 25-27—American Petroleum Institute (API) Pipeline Conference and Cybernetics Symposium—Fort Worth, TX; Contact Madeleine Sellouk, Phone: +1 202/682-8332; E-mail: sellouk@api.org; Web site: www.api.org.

May 1-4—AISTech 2006—The Iron and Steel Technology Conference and Exposition—Cleveland, OH; Contact AIST, Phone: +1 724/776-6040; E-mail: custserv@aist.org; Web site: www.aist.org.

* **May 2-4—40th Annual Western States Corrosion Seminar—Pomona, CA;** Contact Sylvia Hall, Phone: +1 323/564-6626; E-mail: info@westernstatescorrosion.org; Web site: www.westernstatescorrosion.org.

* Sponsored or cosponsored by NACE International.

May 2-4—American Gas Association Operations Conference—Boston, MA; Contact Larry Ingels, Phone: +1 202/824-7336; E-mail: lingels@aga.org; Web site: www.aga.org.

May 7-11—International Conference on Shape Memory and Superelastic Technologies—Pacific Grove, CA; Contact ASM Customer Service, Phone: +1 440/338-5151, ext. 6; E-mail: cust-srv@asminternational.org; Web site: www.asminternational.org.

* **May 10-11—Israeli 7th Conference on Corrosion and Electrochemistry—Ramat Gan, Israel;** Contact Alec Groysman, Phone: +972 4 8788623; E-mail: galec@orl.co.il; Web site: www.engineers.org.il/Index.asp?CategoryID=1122.

* **May 10-11—NACE Pipeline Seminar Series: Internal Corrosion: Tools, Technologies, and Case Studies—Houston, TX;** Contact Helena Seelinger, Phone: +1 281/228-6220; E-mail: helena.seelinger@nace.org.

May 10-12—5th International Conference on NDE in Relation to Structural Integrity for Nuclear and Pressurized Components—San Diego, CA; Contact Brent Lancaster, Phone: +1 704/547-6017; E-mail: blancast@epri.com; Web site: www.epri.com.

* **May 10-12—Pipeline Integrity Management Seminar (PIMS)—New Orleans, LA;** Contact NACE, Phone: +1 281/228-6223; E-mail: firstservice@nace.org.

May 15-18—International Thermal Spray Conference and Exposition (ITSC)—Seattle, WA; Contact ASM Customer Service, Phone: +1 440/338-5151, ext. 6; E-mail: cust-srv@asminternational.org; Web site: www.asminternational.org.

* **May 21-26—LATINCORR 2006—Fortaleza, Ceara, Brazil;** Contact ABRACO, Phone: +55 21 2516 1962; E-mail: eventos@abraco.org.br; Web site: www.abraco.org.br/latincorr2006.

May 30-June 2—7th Congress of CEOCOR—Mondorf-les-Bains, Luxembourg; Contact Congress Secretariat, Phone: +352 31 05 02 201/202; Web site: www.ceocor.lu/luxembourg.

June 5-9—International Gas Union, 23rd World Gas Conference—Amsterdam, Netherlands; Contact WGC2006 Conference and Exhibition Secretariat, Phone: +31 20 6793411; E-mail: wgc2006@eurocongres.com.

* **June 20-22—Offshore Materials and Corrosion: 40 Years On—Edinburgh, Scotland, UK;** Contact Jean Tuck, Phone: +44 (0) 1889 568090; E-mail: mcf@marinecorrosionforum.org; Web site: www.marinecorrosionforum.org.